Chimeralike states in networks of bistable time-delayed feedback oscillators coupled via the mean field

V. I. Ponomarenko,[1,2] D. D. Kulminskiy,[1,2] and M. D. Prokhorov[1]

[1]*Saratov Branch of Kotel'nikov Institute of Radio Engineering and Electronics of Russian Academy of Sciences, Zelyonaya Street, 38, Saratov 410019, Russia*

[2]*Department of Nano- and Biomedical Technologies, Saratov State University, Astrakhanskaya Street, 83, Saratov, 410012, Russia*

(Received 31 March 2017; revised manuscript received 19 June 2017; published 21 August 2017)

We study the collective dynamics of oscillators in a network of identical bistable time-delayed feedback systems globally coupled via the mean field. The influence of delay and inertial properties of the mean field on the collective behavior of globally coupled oscillators is investigated. A variety of oscillation regimes in the network results from the presence of bistable states with substantially different frequencies in coupled oscillators. In the physical experiment and numerical simulation we demonstrate the existence of chimeralike states, in which some of the oscillators in the network exhibit synchronous oscillations, while all other oscillators remain asynchronous.

DOI: 10.1103/PhysRevE.96.022209

I. INTRODUCTION

The spatiotemporal dynamics of networks of coupled oscillators has been intensively studied by many authors for several decades. These investigations have revealed many nonlinear phenomena, including the formation of various structures, clusterization, and synchronization of oscillators in the network [1–3]. It was believed for a long time that the regions of synchronous behavior of network elements can coexist with the regions of asynchronous behavior only in heterogeneous networks, in which oscillators with close frequencies become synchronized, while oscillators with appreciably different frequencies exhibit asynchronous dynamics. Afterwards, it was found out that coexistence of synchronous and asynchronous groups of oscillators is possible also in networks of coupled identical oscillators [4]. Such state was named in Ref. [5] as the chimera state.

Chimera states were first discovered in a network of nonlocally coupled identical phase oscillators [5]. Since then, chimera states have been found in networks with local coupling (only to nearest neighbors) of oscillators [6,7] and networks of globally coupled oscillators [8–10]. Besides the networks of phase oscillators, chimera states can occur in networks composed of other types of oscillators [11–17] and in coupled map lattices [18,19]. Chimera states have been shown to be robust against inhomogeneities of the local dynamics of oscillators [20,21]. In recent years, a lot of theoretical and numerical studies have been devoted to chimera states [22–31].

Chimera states have also been observed in various experiments [32–40]. For example, they have been found in a spatial light modulator feedback system [32], populations of coupled chemical oscillators [33], mechanical systems of metronomes [34,35], experimental realization of a modified Ikeda time-delayed equation [36], chains of electronic circuits with neuronlike spiking dynamics [37,38], an optoelectronic delayed-feedback system [39], and a network of coupled chaotic optoelectronic oscillators [40].

In the present paper, we investigate experimentally and numerically the collective dynamics of oscillators, including chimera states, in a network of identical bistable oscillators with time-delayed feedback globally coupled via the mean field. Global coupling leading to synchronization of oscillators is typical in systems of various natures, including groups of insects [41], living cells [42], hand-clapping individuals in a large audience [43], pedestrians on footbridges [44], electrochemical oscillators [45], and many others. As for time delays, they are inherent in many real-world systems [46,47]. We consider different ways of formation of the mean field and study the influence of delay and inertial properties of the mean field on the collective dynamics of globally coupled oscillators.

In experimental studies, we implemented time-delayed feedback oscillators as electronic time-delay systems. In contrast to experiments dealing with a single electronic time-delay system in Refs. [36,39], we examine a network composed of eight experimental electronic delayed-feedback oscillators globally coupled via the mean field. A network consisting of six electronic time-delay systems coupled via the mean field has been studied experimentally in Ref. [48]. In the present paper, we investigate an experimental scheme that is different from the scheme considered in Ref. [48] and exploits another type of forcing the oscillators by the mean field.

The paper is organized as follows. In Sec. II, we describe the object of investigation representing a network of identical bistable time-delay systems coupled via the mean field and consider the oscillation regimes in this network for different ways of the mean field formation. In Sec. III, the results of the network experimental investigation are presented for the case where the network elements represent electronic self-sustained oscillators with time-delayed feedback. Section IV presents the results of numerical simulation of collective dynamics of oscillators in the network under study. The results are summarized in Sec. V.

II. NETWORK OF TIME-DELAY SYSTEMS COUPLED VIA THE MEAN FIELD

We consider a network consisting of coupled identical time-delay systems, with each system described in the absence of coupling by the following delay-differential equation:

$$\varepsilon \dot{x}(t) = -x(t) + f[x(t-\tau)], \tag{1}$$

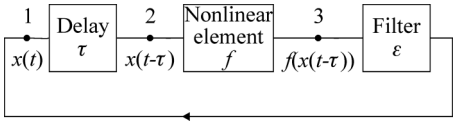

FIG. 1. Block diagram of a ring system with time-delayed feedback. Numerals 1, 2, and 3 designate points where an external signal can be fed into the system.

where τ is the delay time, the parameter ε characterizes the inertial properties of the system, and f is a nonlinear function. In the general case, Eq. (1) is a mathematical model of an oscillating system composed of a ring with three ideal elements: nonlinear, inertial, and delay (Fig. 1).

Let the nonlinear element in the oscillator have a cubic function:

$$f(x) = a + b(x - d) - c(x - d)^3. \tag{2}$$

The function (2) is plotted in Fig. 2 for $a = 1.5$, $b = 2.3$, $c = 1.78$, and $d = 1.57$. With this nonlinearity, the system (1) shows bistability. Depending on the initial conditions, it can exhibit two regimes of oscillations, which occur in the vicinity of unstable fixed points A and B (Fig. 2). Nearby the fixed point A, periodic oscillations in the fundamental mode take place at a frequency close to $\nu_1 = 1/(2\tau)$. Nearby the fixed point B, chaotic oscillations at the third harmonic of the fundamental mode take place at a basic frequency close to $\nu_2 = 3/(2\tau)$. Typical time series of such oscillations in the region of bistability will be considered below. Qualitatively similar regimes of periodic and chaotic oscillations are observed in a time-delay system (1) with a sinusoidal nonlinearity. A detailed investigation of oscillation regimes corresponding to the fundamental solution and higher-harmonic solutions of delay-differential equation (1) with a sine function f has been carried out in Ref. [49].

We couple the oscillators (1) via the mean field $G(t)$, which acts on each element in the network and provides global coupling. The signal $G(t)$ can be fed into the ring

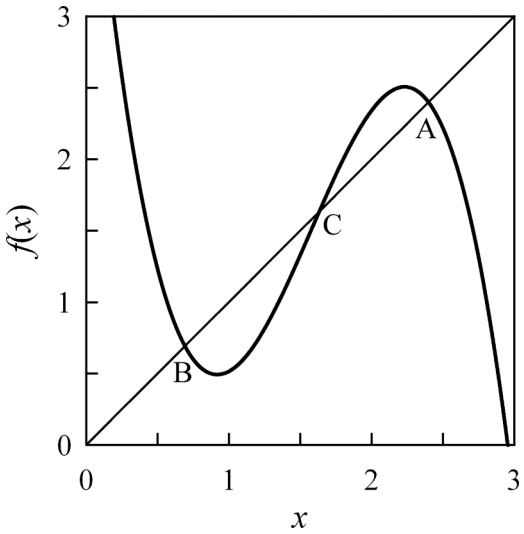

FIG. 2. Plot of function (2) for $a = 1.5$, $b = 2.3$, $c = 1.78$, and $d = 1.57$. A, B, and C are unstable fixed points.

delayed-feedback oscillator at various points [50] indicated by numerals 1, 2, and 3 in Fig. 1. Depending on the point at which the mean field acts on oscillators, their dynamics is described by one of the following equations:

$$\varepsilon\dot{x}_i(t) = -x_i(t) + f[x_i(t - \tau) + kG(t - \tau)], \tag{3}$$

$$\varepsilon\dot{x}_i(t) = -x_i(t) + f[x_i(t - \tau) + kG(t)], \tag{4}$$

$$\varepsilon\dot{x}_i(t) = -x_i(t) + f[x_i(t - \tau)] + kG(t), \tag{5}$$

where $i = 1, \ldots, N$, with N being the number of oscillators, and k is the strength of coupling. The oscillators are governed by Eq. (3), if the signal $G(t)$ acts on these oscillators at point 1. Equations (4) and (5) describe the network oscillators for the cases where $G(t)$ is fed at points 2 and 3, respectively.

In the simplest case, the mean field is formed by the summation of signals $x_i(t)$ from all oscillators and normalization of the summary signal to N:

$$G(t) = \frac{1}{N}\sum_{i=1}^{N} x_i(t). \tag{6}$$

The type of oscillation regime in the considered network is determined by initial conditions in coupled oscillators. If we specify the initial conditions in such a way that some of the oscillators perform oscillations in the fundamental mode (first harmonic), while the other oscillators perform oscillations at the third harmonic of the fundamental mode, then the oscillators in the network will be separated into two clusters, which differ by the frequency of oscillations. The value of phase shift $\Delta\varphi$ between the signals $G(t)$ and $x_i(t)$ determines the collective behavior of oscillators in the network. For $|\Delta\varphi| < \pi/2$, the coupling via the mean field is attractive and the oscillators synchronize between themselves after a transient process, while for $\pi/2 < |\Delta\varphi| < 3\pi/2$, the coupling is repulsive and the oscillators remain asynchronous [8,51].

Let us consider the case where the signal $G(t)$ acts on the network oscillators at point 1 (Fig. 1) affecting the variable $x_i(t)$. If the mean field is described by Eq. (6), the phase shift between the signals $G(t)$ and $x_i(t)$ is absent ($\Delta\varphi = 0$) and oscillators are synchronized both in the first and in the second clusters.

In general case, the mean field can be formed in a complicated way. For example, a medium that couples the oscillators can possess inertial properties or have its own delay induced by finite velocity of signal propagation and processing. A complication of the mean field signal may result in greater diversity of oscillation regimes in the network of coupled oscillators.

First, we consider the influence of the mean field inertial properties on the collective dynamics of coupled oscillators described by Eq. (3). Assume that inertial properties of the mean field are due to a linear filtering of the summary signal (6) by a low-pass first-order filter, and the mean field is described by the following equation:

$$\gamma\dot{G}(t) + G(t) = \frac{1}{N}\sum_{i=1}^{N} x_i(t), \tag{7}$$

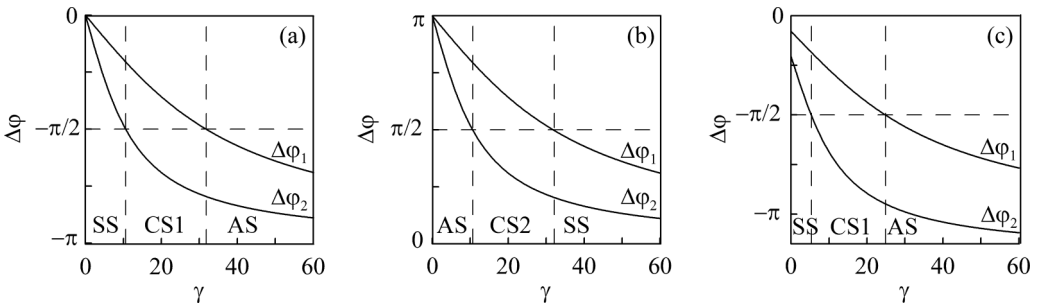

FIG. 3. Dependencies $\Delta\varphi_1(\gamma)$ and $\Delta\varphi_2(\gamma)$ described by Eqs. (11) and (12) (a), Eqs. (13) and (14) (b), and Eqs. (15) and (16) (c) for $\nu_1 = 1/200$ and $\nu_2 = 3/200$. Regions with synchronous behavior of oscillators in both clusters are denoted by SS. Regions with asynchronous behavior of oscillators in both clusters are denoted by AS. Regions in which chimeralike states take place are denoted by CS1 and CS2.

where $\gamma = 1/f_F$ is the time constant of the filter and f_F is the filter cutoff frequency. Since all oscillators in the network take part in the formation of the mean field, the signal (6) has two main components with the frequencies close to ν_1 and ν_2. Each of these components, as it passes through a linear low-pass first-order filter, undergoes a phase shift,

$$\Delta\varphi = -\arctan(2\pi\nu\gamma), \tag{8}$$

whose value depends on the frequency ν. For the low-frequency component of $G(t)$, $\nu = \nu_1$ and $\Delta\varphi = \Delta\varphi_1$ in Eq. (8), while for the high-frequency component of $G(t)$, $\nu = \nu_2$ and $\Delta\varphi = \Delta\varphi_2$.

Since for the phase shift $\Delta\varphi$ defined by Eq. (8) the condition $|\Delta\varphi| < \pi/2$ is always fulfilled, the coupling via the mean field is attractive for the oscillators in both clusters. Therefore, the oscillators in the first cluster become synchronized as well as the oscillators in the second cluster.

Let us consider a more complicated situation, in which one filter is not enough for modeling the inertial properties of the mean field. Assume that inertial properties of the mean field are due to a linear filtering of the summary signal (6) by two series-connected low-pass first-order filters, and the mean field is described by the following equation:

$$\gamma_1\gamma_2\ddot{G}(t) + (\gamma_1 + \gamma_2)\dot{G}(t) + G(t) = \frac{1}{N}\sum_{i=1}^{N} x_i(t), \tag{9}$$

where $\gamma_1 = 1/f_{F1}$ and $\gamma_2 = 1/f_{F2}$ are the time constants of the filters and f_{F1} and f_{F2} are the cutoff frequencies for the first and second filter, respectively. If $\gamma_1 = \gamma_2 = \gamma$, Eq. (9) may be written as follows:

$$\gamma^2\ddot{G}(t) + 2\gamma\dot{G}(t) + G(t) = \frac{1}{N}\sum_{i=1}^{N} x_i(t). \tag{10}$$

Under this filtering, the signal (6) components with the frequencies close to ν_1 and ν_2 undergo the phase shifts $\Delta\varphi_1$ and $\Delta\varphi_2$, respectively:

$$\Delta\varphi_1 = -2\arctan(2\pi\nu_1\gamma), \tag{11}$$

$$\Delta\varphi_2 = -2\arctan(2\pi\nu_2\gamma). \tag{12}$$

For the phase shifts (11) and (12), the condition $|\Delta\varphi_{1,2}| < \pi$ is always fulfilled. In the case $\pi/2 < |\Delta\varphi_{1,2}| < \pi$, the coupling via the mean filed is repulsive and oscillators exhibit asynchronous behavior. Figure 3(a) shows the dependencies $\Delta\varphi_1(\gamma)$ and $\Delta\varphi_2(\gamma)$ for $\tau = 100$ ($\nu_1 = 1/200$ and $\nu_2 = 3/200$). Since $\nu_1 < \nu_2$, the phase shift (11) is less by the absolute value than the phase shift (12). Depending on γ, three qualitatively different situations can take place: (i) $|\Delta\varphi_1| < \pi/2$ and $|\Delta\varphi_2| < \pi/2$, (ii) $|\Delta\varphi_1| < \pi/2$ and $\pi/2 \leqslant |\Delta\varphi_2| < \pi$, and (iii) $\pi/2 \leqslant |\Delta\varphi_1| < \pi$ and $\pi/2 \leqslant |\Delta\varphi_2| < \pi$. In Fig. 3(a), the regions corresponding to these three situations are denoted by SS, CS1, and AS, respectively.

For γ values from the SS region, synchronization is observed between oscillators in the first cluster and between oscillators in the second cluster. In the AS region, the oscillators in both clusters exhibit asynchronous oscillations. In the CS1 region, the oscillators in the first cluster performing oscillations in the fundamental mode exhibit synchronous behavior, while the oscillators in the second cluster performing oscillations at the third harmonic of the fundamental mode exhibit asynchronous behavior. This situation corresponds to a chimeralike state, in which a cluster with synchronized oscillators coexists with a cluster with desynchronized oscillators. It should be noted that according to Refs. [8,13], this type of oscillation regime in a network of globally coupled oscillators should be called a chimeralike state rather than a chimera state, since it is reminiscent of the typical chimera state [4,5] under the nonlocal coupling.

If the signal $G(t)$ is fed into the network oscillators at point 2 (Fig. 1), it affects the variable $x_i(t-\tau)$. Under this forcing, a phase shift between the signals $G(t)$ and $x_i(t)$ is present. The value of this phase shift is about π for the oscillations in the fundamental mode and about 3π for the oscillations at the third harmonic of the fundamental mode. This phase shift should be taken into account at calculating the total phase shift between the signals $G(t)$ and $x_i(t)$ in the presence of inertial properties of the mean field. Since the phase shift is a periodic function with the period 2π, Eqs. (11) and (12) take the following form:

$$\Delta\varphi_1 = -2\arctan(2\pi\nu_1\gamma) + \pi, \tag{13}$$

$$\Delta\varphi_2 = -2\arctan(2\pi\nu_2\gamma) + \pi. \tag{14}$$

The dependencies $\Delta\varphi_1(\gamma)$ and $\Delta\varphi_2(\gamma)$ described by Eqs. (13) and (14) are constructed in Fig. 3(b) for $\nu_1 = 1/200$ and $\nu_2 = 3/200$. Depending on γ, three different situations

can take place: (i) $|\Delta\varphi_1| < \pi/2$ and $|\Delta\varphi_2| < \pi/2$, (ii) $\pi/2 \leqslant |\Delta\varphi_1| < \pi$ and $|\Delta\varphi_2| < \pi/2$, and (iii) $\pi/2 \leqslant |\Delta\varphi_1| < \pi$ and $\pi/2 \leqslant |\Delta\varphi_2| < \pi$. In Fig. 3(b), the regions corresponding to these three situations are designated as SS, CS2, and AS, respectively. For γ values from the CS2 region, a chimeralike state is observed. However, in contrast to the chimeralike state in the region CS1 [Fig. 3(a)], the oscillators in the first cluster performing oscillations in the fundamental mode exhibit asynchronous behavior, while the oscillators in the second cluster performing oscillations at the third harmonic of the fundamental mode exhibit synchronous behavior.

In the case where the signal $G(t)$ acts on the oscillators at point 3 (Fig. 1), the phase shifts $\Delta\varphi_1$ and $\Delta\varphi_2$ are described by the following equations:

$$\Delta\varphi_1 = -2\arctan(2\pi\nu_1\gamma) - \arctan(2\pi\nu_1\varepsilon), \quad (15)$$

$$\Delta\varphi_2 = -2\arctan(2\pi\nu_2\gamma) - \arctan(2\pi\nu_2\varepsilon). \quad (16)$$

Figure 3(c) shows the dependencies $\Delta\varphi_1(\gamma)$ and $\Delta\varphi_2(\gamma)$ described by Eqs. (15) and (16) for $\nu_1 = 1/200$, $\nu_2 = 3/200$, and $\varepsilon = 8$. Similarly to Fig. 3(a), there are three regions denoted by SS, CS1, and AS in Fig. 3(c), in which the synchronous regime, chimeralike state, and asynchronous regime, respectively, take place.

Let us consider now the influence of delay in the mean field on the collective dynamics of coupled oscillators described by Eq. (3). Assume that the mean field is described as follows:

$$G(t) = \frac{1}{N}\sum_{i=1}^{N} x_i(t - \tau_m), \quad (17)$$

where τ_m is the delay time of the mean field. The phase shifts $\Delta\varphi_1$ and $\Delta\varphi_2$ for both components of $G(t)$ corresponding to oscillations in the fundamental mode and oscillations at the third harmonic of the fundamental mode, respectively, have a linear dependence on τ_m:

$$\Delta\varphi_1 = -2\nu_1\tau_m, \quad (18)$$

$$\Delta\varphi_2 = -2\nu_2\tau_m. \quad (19)$$

Figure 4 shows the dependencies $\Delta\varphi_1(\tau_m)$ and $\Delta\varphi_2(\tau_m)$ for $\nu_1 = 1/200$ and $\nu_2 = 3/200$. Depending on τ_m, four different regions are identified in Fig. 4 designated as SS, CS1, CS2, and AS. In the presence of delay in the mean field, two different chimeralike states (one in region CS1 and another in region CS2) can take place in the network in contrast to the case considered above, in which only one chimeralike state is observed in the network. Note that for the oscillators in the second cluster performing oscillations at the third harmonic of the fundamental mode, the coupling is repulsive for $\pi/2 < |\Delta\varphi_2| < 3\pi/2$ and attractive for $3\pi/2 < |\Delta\varphi_2| < 5\pi/2$. Since the phase is a periodic function with the period 2π, the last relation is equivalent to the relation $|\Delta\varphi_2| < \pi/2$.

Thus the collective dynamics of oscillators globally coupled via the mean field depends on the delay and inertial properties of the mean field. If we have a possibility to vary the parameters of the mean field, then we can control the behavior of

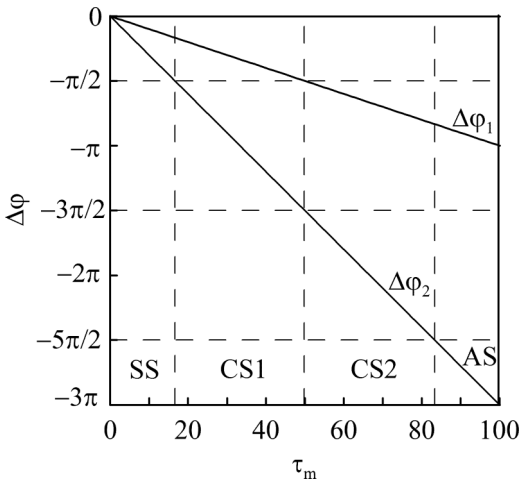

FIG. 4. Dependencies $\Delta\varphi_1(\tau_m)$ and $\Delta\varphi_2(\tau_m)$ for $\nu_1 = 1/200$ and $\nu_2 = 3/200$. Regions with synchronous behavior of oscillators in both clusters are denoted by SS. Regions with asynchronous behavior of oscillators in both clusters are denoted by AS. Regions in which chimeralike states take place are denoted by CS1 and CS2.

oscillators in clusters, including the formation of chimeralike states. In the general case, the mean field can possess both delay and inertial properties, but we do not consider this situation in the present paper.

III. EXPERIMENTAL RESULTS

We study experimentally a network composed of eight bistable time-delay systems described in the absence of coupling by Eq. (1). Each element in the network represents a ring electronic oscillator with time-delayed feedback. In the block representation of this oscillator (Fig. 1), a delay for time τ is provided by a delay line, the role of a nonlinear element is played by an amplifier with the transfer function f, and the system inertial properties are defined by a low-pass first-order RC filter, whose parameters specify ε. For this oscillator, $x(t)$ and $x(t - \tau)$ in Eq. (1) are the voltages at the delay line input and output, respectively, and $\varepsilon = RC$, where R is the resistance and C is the capacitance.

Our electronic oscillators contain an analog RC filter and digital delay line and a nonlinear element implemented on programmable microcontrollers. We used 32-bit Atmel microcontrollers based on the ARM Cortex-M3 processor. The analog and digital elements of the oscillators are connected with the help of analog-to-digital converters and digital-to-analog converters.

A block diagram of the network of coupled oscillators under investigation is depicted in Fig. 5. The mean field is formed by the summation of signals $x_i(t)$ from all oscillators using the summing amplifier with the transfer coefficient k and normalization of the summary signal to N. The resulting signal passes through a linear phase-shifting chain comprising two series-connected low-pass first-order RC filters. In this case, the mean field $G(t)$ is described by Eq. (9), where $\gamma_1 = R_1C_1$ and $\gamma_2 = R_2C_2$. The signal $G(t)$ is fed into each oscillator between the filter and delay line as an external forcing. This type of forcing corresponds to the case where $G(t)$ acts on the

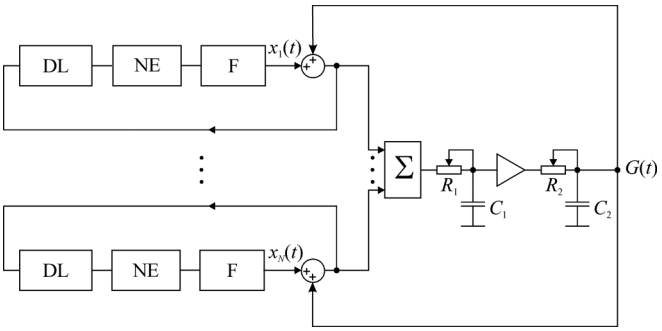

FIG. 5. Block diagram of a network of time-delayed feedback oscillators globally coupled via the mean field. The first and Nth oscillators are depicted. The delay lines, nonlinear elements, and filters are denoted by DL, NE, and F, respectively. The summary amplifier is denoted by Σ.

network oscillators at point 1 (Fig. 1). In this case, the coupled oscillators are governed by Eq. (3).

The parameters of the oscillators are $\tau = 1$ ms and $\varepsilon = 0.08$ ms and the transfer function is described by cubic function (2) depicted in Fig. 2. The transfer coefficient of the summing amplifier is $k = 0.01$. By programming the microcontrollers, we specify the initial conditions as a constant value on the time interval equal to τ. For four oscillators, the initial conditions are set equal to 2 V, while for the four other oscillators they are set equal to 0.5 V. These initial conditions fall into the basin of attraction of periodic and chaotic attractor, respectively. As a result, four oscillators perform periodic oscillations in the fundamental mode, while the four other oscillators perform chaotic oscillations at the third harmonic of the fundamental mode. In this case, the oscillators in the network are separated into two clusters. One of these clusters contains oscillators with periodic behavior at a frequency close to ν_1 and another cluster contains oscillators with chaotic dynamics at a basic frequency close to ν_2.

Varying the values of resistors R_1 and R_2 (Fig. 5), we change the phase shifts $\Delta\varphi_1$ and $\Delta\varphi_2$ and observe three qualitatively different situations: (i) $|\Delta\varphi_1| < \pi/2$ and $|\Delta\varphi_2| < \pi/2$, (ii) $|\Delta\varphi_1| < \pi/2$ and $\pi/2 \leqslant |\Delta\varphi_2| < \pi$, and (iii) $\pi/2 \leqslant |\Delta\varphi_1| < \pi$ and $\pi/2 \leqslant |\Delta\varphi_2| < \pi$, described in Sec. II.

In the first case, synchronization takes place between periodic oscillators in the first cluster and between chaotic oscillators in the second cluster. Figure 6(a) shows parts of the experimental time series of voltage in eight coupled oscillators for $|\Delta\varphi_1| = 0.002\pi$ and $|\Delta\varphi_2| = 0.006\pi$. As seen in Fig. 6(a), the time series of periodic oscillators are slightly different. It is explained by the fact that it is practically impossible to ensure the absolute identity of analog RC filters in experimental electronic oscillators. In the ideal case of identical oscillators, one would observe complete synchronization of periodic oscillators (see Sec. IV). The chaotic oscillators in Fig. 6(a) exhibit phase synchronization, but the amplitude of oscillations can be different.

The second situation is illustrated in Fig. 6(b) showing parts of the time series of voltage in all coupled oscillators for $|\Delta\varphi_1| = 0.47\pi$ and $|\Delta\varphi_2| = 0.51\pi$. The periodic oscillators exhibit synchronization similar to the case depicted in Fig. 6(a). The chaotic oscillators exhibit asynchronous

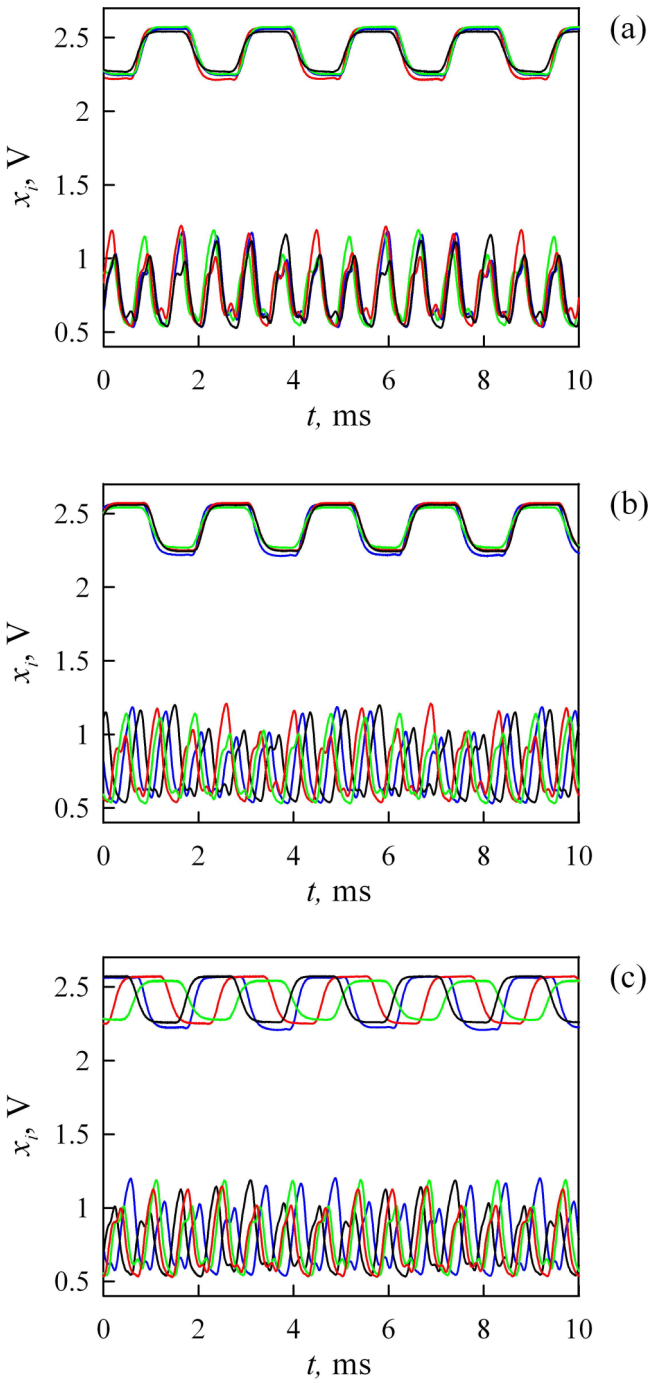

FIG. 6. Experimental time series of voltage in eight coupled electronic oscillators for $|\Delta\varphi_1| = 0.002\pi$ and $|\Delta\varphi_2| = 0.006\pi$ (a), $|\Delta\varphi_1| = 0.47\pi$ and $|\Delta\varphi_2| = 0.51\pi$ (b), and $|\Delta\varphi_1| = 0.8\pi$ and $|\Delta\varphi_2| = 0.99\pi$ (c). The time series of periodic and chaotic oscillators are shown at the top and at the bottom of the figures, respectively. The same set of colors is used for both periodic and chaotic time series.

behavior. This situation corresponds to a chimeralike state. It should be noted that chimeralike states are identified in the considered network in spite of the employment of only eight coupled oscillators. As it was shown recently in Refs. [40,52–55], chimera states can be identified even in small networks

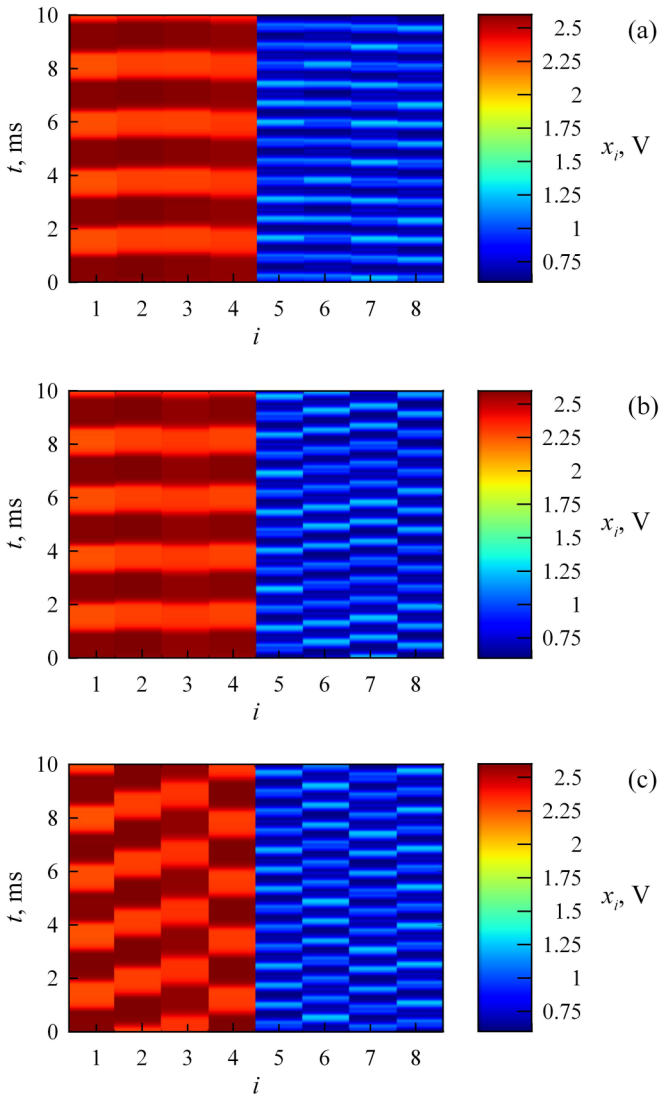

FIG. 7. Space-time plots of the network of eight coupled experimental oscillators for $|\Delta\varphi_1| = 0.002\pi$ and $|\Delta\varphi_2| = 0.006\pi$ (a), $|\Delta\varphi_1| = 0.47\pi$ and $|\Delta\varphi_2| = 0.51\pi$ (b), and $|\Delta\varphi_1| = 0.8\pi$ and $|\Delta\varphi_2| = 0.99\pi$ (c).

of coupled oscillators. Only four identical coupled oscillators are sufficient for observation of chimera states [40,52,54].

The last situation is illustrated in Fig. 6(c). This figure shows parts of the time series of voltage in eight coupled oscillators for $|\Delta\varphi_1| = 0.8\pi$ and $|\Delta\varphi_2| = 0.99\pi$. In this case, the oscillators in both clusters exhibit asynchronous behavior.

Figure 7 shows the space-time plots of the network of eight coupled experimental electronic oscillators for each of the three situations depicted in Fig. 6. The oscillators performing periodic oscillations are denoted by the numbers from 1 to 4, while the oscillators performing chaotic oscillations are denoted by the numbers from 5 to 8. Since the analog *RC* filters in the real oscillators cannot be absolutely identical, the periodic oscillators 1–4 exhibit slightly different oscillations even in the synchronous regimes [Figs. 7(a) and 7(b)]. In Fig. 7(a), the chaotic oscillators 5–8 exhibit phase synchronization, but the amplitude of oscillations can be different. In Figs. 7(b) and 7(c), the chaotic oscillators exhibit asynchronous behavior. In this case, the difference between the amplitudes of their oscillations is more pronounced than in Fig. 7(a).

For the other ratios between the number of periodic oscillators and the number of chaotic oscillators in the network, we observed qualitatively similar collective dynamics of coupled oscillators. We could identify chimeralike states in the network of eight coupled experimental electronic oscillators, if the number of the network elements performing periodic (or chaotic) oscillations was from two to six.

In our recent paper [48], we studied experimentally a network composed of six electronic oscillators with time-delayed feedback coupled via the mean field, which was fed into oscillators between the nonlinear element and filter. This type of forcing corresponds to the case where $G(t)$ acts on the ring oscillators at point 3 (Fig. 1), and the coupled oscillators are modeled by Eq. (5). In this network, we have observed the oscillation regimes qualitatively similar to those mentioned above for the scheme depicted in Fig. 5.

IV. RESULTS OF NUMERICAL SIMULATION

We have also carried out numerical simulation of collective dynamics of oscillators in networks of identical bistable time-delay systems coupled via the mean field. To compare the results of modeling with those of physical experiment presented in Sec. III, we consider a network consisting of eight bistable time-delayed feedback oscillators described by Eq. (3) with $\tau = 100$, $\varepsilon = 8$, and $k = 0.01$ and coupled via the mean field $G(t)$ described by Eq. (9). The nonlinear function of the oscillators is described by Eq. (2) with the same parameter values as in the physical experiment (see Fig. 2).

Depending on the initial conditions, the oscillators can perform either periodic oscillations in the fundamental mode at a frequency close to ν_1 or chaotic oscillations at the third harmonic of the fundamental mode at a basic frequency close to $\nu_2 = 3\nu_1$. Similarly to the physical experiment, one can specify the initial conditions as a constant value on the time interval equal to τ. For example, if the initial conditions are set equal to 0.5, the oscillator exhibits chaotic oscillations in the vicinity of the fixed point B (Fig. 2). If the initial conditions are set equal to 2, the oscillator exhibits periodic oscillations in the vicinity of the fixed point A. Thus the number p of periodic oscillators and the number n of chaotic oscillators in the network are fully determined by initial conditions.

In the network consisting of N bistable oscillators, depending on the initial conditions, $N + 1$ different regimes can take place, in which n and p take the values from 0 to N, with $n + p = N$. For $p = 0$ and $p = N$, only one cluster is formed in the network, which consists of chaotic or periodic oscillators, respectively. Depending on the value of phase shift between the signals $G(t)$ and $x_i(t)$, the oscillators in this cluster exhibit either synchronous or asynchronous behavior. For $p = 1, \ldots, N-1$, the network contains both periodic and chaotic oscillators. However, for $p = 1$ and $p = N - 1$, there is only one periodic or only one chaotic oscillator, respectively, for which the notion of synchronous or asynchronous collective dynamics does not make sense. Therefore, chimeralike states are not observed at $p = 1$ and $p = N - 1$. In the considered network of $N = 8$ bistable oscillators, we could identify chimeralike states for $p = 2, \ldots, 6$.

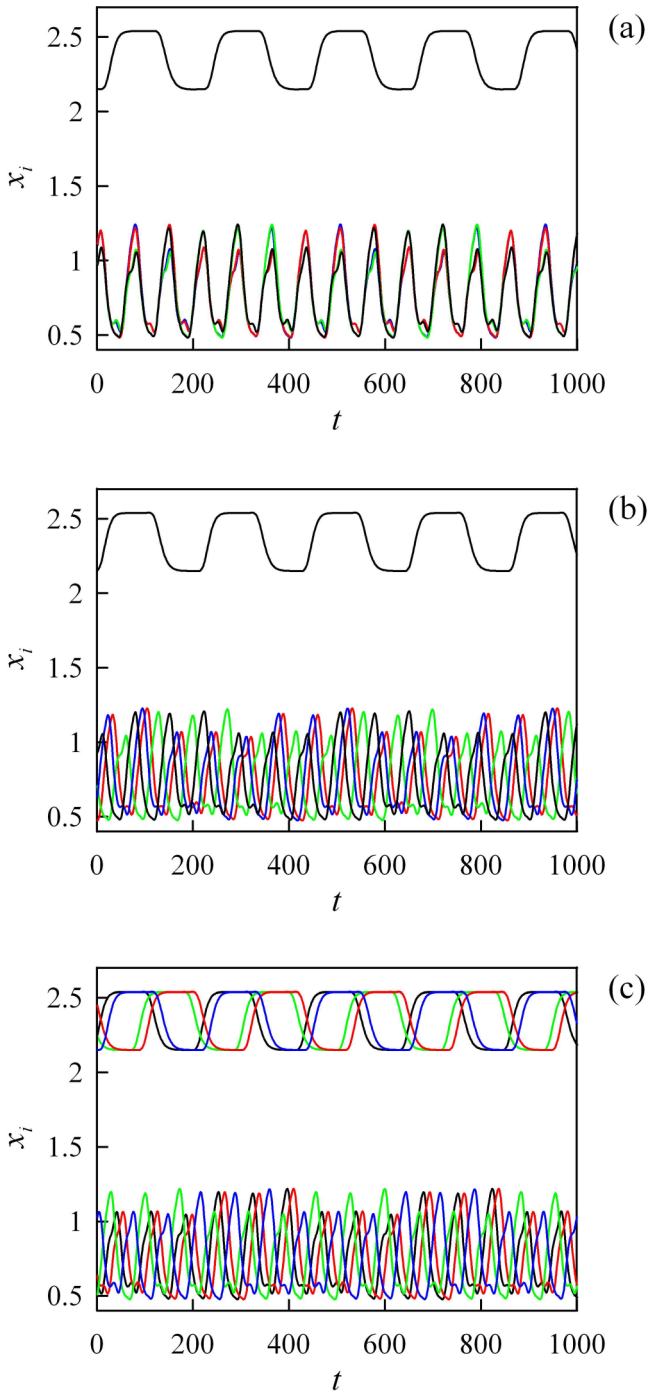

FIG. 8. Time series of oscillations in the coupled model time-delay systems (3) for $|\Delta\varphi_1| = 0.04\pi$ and $|\Delta\varphi_2| = 0.12\pi$ (a), $|\Delta\varphi_1| = 0.36\pi$ and $|\Delta\varphi_2| = 0.69\pi$ (b), and $|\Delta\varphi_1| = 0.64\pi$ and $|\Delta\varphi_2| = 0.87\pi$ (c).

The initial conditions in the network oscillators can be specified in a random way. For random choice of initial conditions in oscillators, we affect each oscillator by independent noise with the uniform distribution on the interval [0.7,2.5]. At such noise, the initial conditions can fall into the basin of attraction of a periodic attractor, as well as into the basin of attraction of a chaotic attractor. When the noise is switched off, we have a random combination of oscillation regimes in the network elements. One subset of the oscillators performs periodic oscillations, while another subset performs chaotic oscillations. By analogy with the real experiment, we consider the case where four elements exhibit periodic oscillations at a frequency close to ν_1, while the four other elements exhibit chaotic oscillations at a basic frequency close to ν_2.

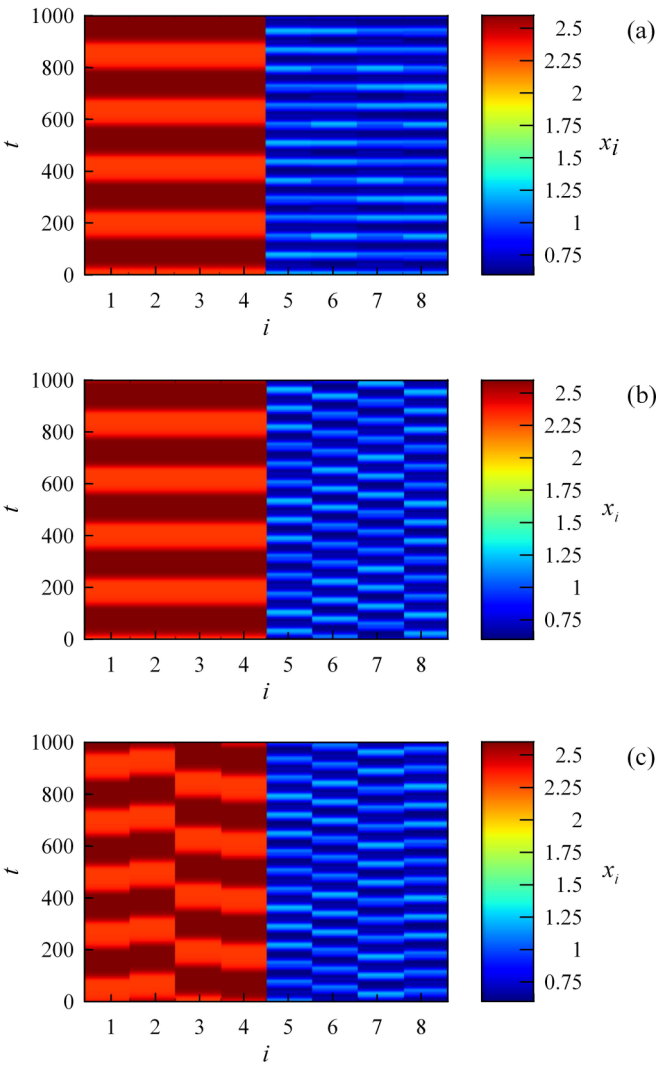

FIG. 9. Space-time plots of the network of eight coupled model oscillators (3) for $|\Delta\varphi_1| = 0.04\pi$ and $|\Delta\varphi_2| = 0.12\pi$ (a), $|\Delta\varphi_1| = 0.36\pi$ and $|\Delta\varphi_2| = 0.69\pi$ (b), and $|\Delta\varphi_1| = 0.64\pi$ and $|\Delta\varphi_2| = 0.87\pi$ (c).

Parts of the time series of $x_i(t)$ in eight coupled model oscillators are shown in Fig. 8 for different values of phase shifts $\Delta\varphi_1$ and $\Delta\varphi_2$. Figure 8(a) illustrates the case where the periodic oscillators are completely synchronized, while the chaotic oscillators exhibit phase synchronization. In contrast to the physical experiment (Fig. 6), all oscillators are absolutely identical. Therefore, the time series of all periodic oscillators in Figs. 8(a) and 8(b) completely coincide and it is not possible to make a distinction between these time series. Figure 8(b) shows a chimeralike state, in which the periodic oscillators are synchronized, while the chaotic oscillators are desynchronized. In Fig. 8(c), both periodic and chaotic oscillators exhibit asynchronous oscillations.

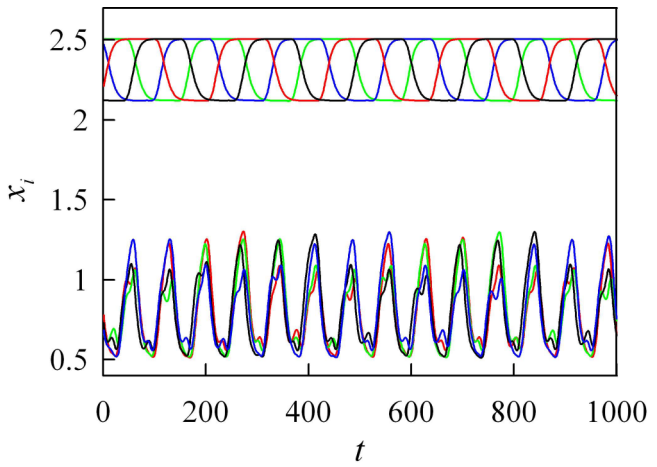

FIG. 10. Time series of oscillations in the coupled model time-delay systems (4) for a chimeralike state for $|\Delta\varphi_1| = 0.72\pi$ and $|\Delta\varphi_2| = 0.40\pi$.

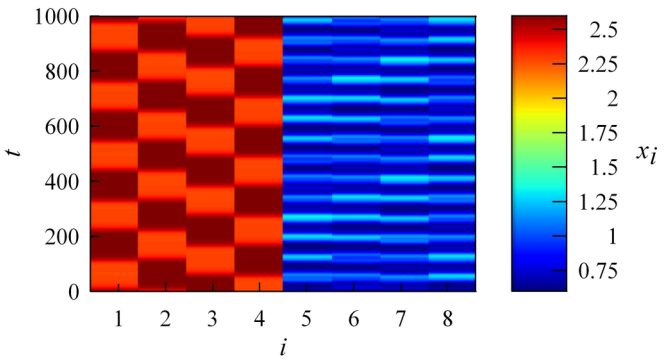

FIG. 11. Space-time plot of the network of eight coupled model oscillators (4) illustrating a chimeralike state for $|\Delta\varphi_1| = 0.72\pi$ and $|\Delta\varphi_2| = 0.40\pi$.

The space-time plots of the model network of coupled oscillators are shown in Fig. 9. The oscillators performing periodic oscillations are denoted by the numbers from 1 to 4, while the oscillators performing chaotic oscillations are denoted by the numbers from 5 to 8. Figure 9 agrees well with Fig. 7 constructed for coupled experimental electronic oscillators. In Fig. 9(a), the periodic oscillators 1–4 exhibit complete synchronization, while the chaotic oscillators 5–8 exhibit phase synchronization. Figure 9(b) illustrates a chimeralike state and Fig. 9(c) shows a situation where both periodic and chaotic oscillators exhibit asynchronous behavior.

It should be noted that if the initial conditions are specified in such a way that the oscillators denoted by the numbers from 1 to 4 in Fig. 9 perform chaotic oscillations, while the oscillators denoted by the numbers from 5 to 8 perform periodic oscillations, then the left and right parts in Fig. 9 will change places. In this case, a chimeralike state will take place, in which the periodic oscillators 5–8 exhibit synchronization, while the chaotic oscillators 1–4 exhibit asynchronous behavior. This situation will be opposite to the situation depicted in Fig. 9(b).

In the general case, the oscillators performing periodic or chaotic oscillations can have any number. For example, the initial conditions can be specified in such a way that the oscillators denoted by the numbers 1, 3, 6, and 7 in Fig. 9 will perform periodic oscillations, while the oscillators denoted by the numbers 2, 4, 5, and 8 will perform chaotic oscillations. Since the elements of the network are not spatially ordered, for the visualization of oscillation regimes in this case, it is convenient to renumber the oscillators with respect to the oscillation regime they display. As a result, we obtain a figure similar to Fig. 9. If the coupling via the mean field is attractive for periodic oscillators and repulsive for chaotic oscillators, a chimeralike state will occur in such network.

For the network consisting of oscillators governed by Eq. (5) and coupled via the mean field $G(t)$ described by Eq. (9), we obtain the results qualitatively similar to those presented in Figs. 8 and 9. We investigate also the network dynamics for the case where the behavior of each oscillator in the network is described by Eq. (4). Depending on the phase shifts $\Delta\varphi_1$ and $\Delta\varphi_2$, different oscillation regimes are observed in the network. We observed a regime in which the periodic oscillators in the first cluster are synchronized and the chaotic oscillators in the second cluster are synchronized, and a regime in which both periodic and chaotic oscillators are desynchronized. Moreover, we identified a chimeralike state that was not observed in the network of coupled oscillators described by Eq. (3). In this regime, the chaotic oscillators exhibit synchronous behavior, while the periodic oscillators exhibit asynchronous behavior. For this chimeralike state, Fig. 10 depicts parts of the time series of $x_i(t)$ in eight coupled oscillators, and Fig. 11 shows the space-time plot of the network. Note that boundaries of the regions with different oscillation regimes in the numerical simulation agree well with the boundaries of the regions in Fig. 3.

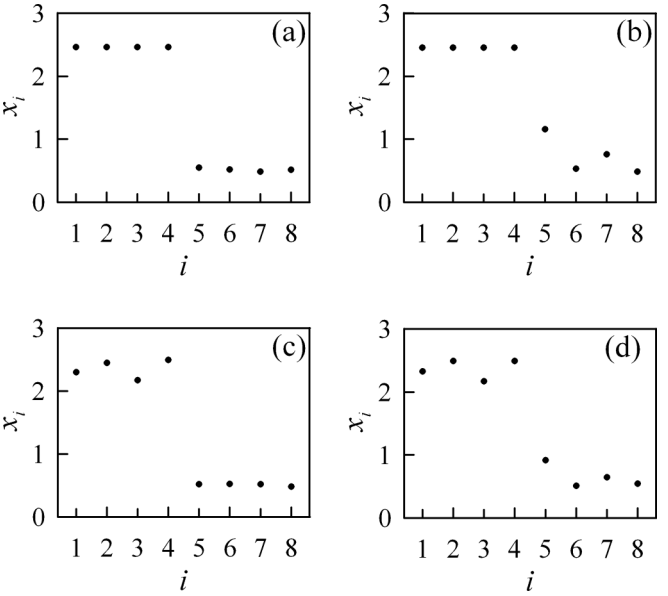

FIG. 12. Snapshots of variables $x_i(t)$ in eight coupled model oscillators (3) in the presence of delay in the mean field for $|\Delta\varphi_1| = 0.05\pi$ and $|\Delta\varphi_2| = 0.15\pi$ (a), $|\Delta\varphi_1| = 0.24\pi$ and $|\Delta\varphi_2| = 0.72\pi$ (b), $|\Delta\varphi_1| = 0.63\pi$ and $|\Delta\varphi_2| = 1.89\pi$ (c), and $|\Delta\varphi_1| = 0.91\pi$ and $|\Delta\varphi_2| = 2.73\pi$ (d).

Finally, we illustrate the collective dynamics of coupled oscillators described by Eq. (3) in the presence of delay in the mean field described by Eq. (17). In accordance with the theoretical results presented in Sec. II, four different oscillation regimes are observed in the network. For each of these regimes, Fig. 12 shows the snapshots of variables $x_i(t)$. The periodic oscillators are denoted by the numbers from 1 to 4, while the chaotic oscillators are denoted by the numbers from 5 to 8.

The regime in which both periodic and chaotic oscillators are synchronized is presented in Fig. 12(a). Figures 12(b) and 12(c) illustrate two different chimeralike states. In the first chimeralike state, the periodic oscillators are synchronized, while the chaotic oscillators are desynchronized [Fig. 12(b)]. In the second chimeralike state, on the contrary, the periodic oscillators are desynchronized, while the chaotic oscillators are synchronized [Fig. 12(c)]. Figure 12(d) shows the regime in which both periodic and chaotic oscillators exhibit asynchronous behavior.

V. CONCLUSION

We have studied the collective dynamics of oscillators in the networks of identical bistable time-delay systems globally coupled via the mean field. Different ways of formation of the mean field are considered. The influence of delay and inertial properties of the mean field on the collective behavior of oscillators is investigated.

The variety of oscillation regimes in the considered networks results from the presence of bistable states with substantially different frequencies in coupled oscillators. One of the bistable regimes takes place in the fundamental mode of the time-delay system oscillations, while another regime takes place at the third harmonic of the fundamental mode. This feature of the bistable system under investigation allows us to ensure different phase shifts of the signal of the mean field for oscillators performing oscillations at different harmonics.

The type of oscillation regime in the network depends on initial conditions in coupled oscillators. The initial conditions can be specified in a required way for each oscillator separately or can be specified in a random way with the help of noise. It is shown that two clusters coexist in the network. Depending on the phase shift of the mean field, each of these clusters can exhibit either synchronous or asynchronous behavior of oscillators in the cluster. In the case where the coupling via the mean field is attractive for oscillators in one cluster and repulsive for oscillators in another cluster, a chimeralike state occurs in the network. In this state, clusters with synchronized and desynchronized oscillators coexist in the network. Thus, varying the parameters of the mean field, it is possible to control the behavior of oscillators in clusters, including the formation of chimeralike states.

We have considered the situation in which oscillators perform periodic oscillations in one of the bistable states and chaotic oscillations in another bistable state. However, qualitatively similar results can be obtained in the cases where both bistable states are periodic or both bistable states are chaotic. It should be noted that in the case of attractive coupling, the identical periodic oscillators exhibit complete synchronization, while the chaotic oscillators exhibit phase synchronization.

We have studied the features of the collective dynamics of oscillators in the network of identical bistable time-delayed feedback systems for the cases where the signal of the mean field is fed into the ring time-delay systems at various points. The similarities and distinctions of these cases are shown.

ACKNOWLEDGMENT

This work was supported by the Russian Foundation for Basic Research, Grant No. 16-02-00091.

[1] V. S. Afraimovich, V. I. Nekorkin, G. V. Osipov, and V. D. Shalfeev, *Stability, Structures, and Chaos in Nonlinear Synchronization Networks* (World Scientific, Singapore, 1995).

[2] A. Pikovsky, M. Rosenblum, and J. Kurths, *Synchronization: A Universal Concept in Nonlinear Sciences* (Cambridge University Press, Cambridge, 2001).

[3] G. V. Osipov, J. Kurths, and C. Zhou, *Synchronization in Oscillatory Networks* (Springer, Berlin, 2007).

[4] Y. Kuramoto and D. Battogtokh, Nonlinear Phenom. Complex Syst. (Minsk, Belarus) **5**, 380 (2002).

[5] D. M. Abrams and S. H. Strogatz, Phys. Rev. Lett. **93**, 174102 (2004).

[6] R. Singh and S. Sinha, Phys. Rev. E **87**, 012907 (2013).

[7] C. R. Laing, Phys. Rev. E **92**, 050904(R) (2015).

[8] A. Yeldesbay, A. Pikovsky, and M. Rosenblum, Phys. Rev. Lett. **112**, 144103 (2014).

[9] L. Schmidt, K. Schönleber, K. Krischer, and V. García-Morales, Chaos **24**, 013102 (2014).

[10] G. C. Sethia and A. Sen, Phys. Rev. Lett. **112**, 144101 (2014).

[11] R. Gopal, V. K. Chandrasekar, A. Venkatesan, and M. Lakshmanan, Phys. Rev. E **89**, 052914 (2014).

[12] V. K. Chandrasekar, R. Gopal, A. Venkatesan, and M. Lakshmanan, Phys. Rev. E **90**, 062913 (2014).

[13] A. Mishra, C. Hens, M. Bose, P. K. Roy, and S. K. Dana, Phys. Rev. E **92**, 062920 (2015).

[14] B. K. Bera, D. Ghosh, and M. Lakshmanan, Phys. Rev. E **93**, 012205 (2016).

[15] N. Semenova, A. Zakharova, V. Anishchenko, and E. Schöll, Phys. Rev. Lett. **117**, 014102 (2016).

[16] S. Ulonska, I. Omelchenko, A. Zakharova, and E. Schöll, Chaos **26**, 094825 (2016).

[17] D. Dudkowski, Y. Maistrenko, and T. Kapitaniak, Chaos **26**, 116306 (2016).

[18] I. Omelchenko, Y. Maistrenko, P. Hövel, and E. Schöll, Phys. Rev. Lett. **106**, 234102 (2011).

[19] D. Dudkowski, Y. Maistrenko, and T. Kapitaniak, Phys. Rev. E **90**, 032920 (2014).

[20] J. Xie, H.-C. Kao, and E. Knobloch, Phys. Rev. E **91**, 032918 (2015).

[21] I. Omelchenko, A. Provata, J. Hizanidis, E. Schöll, and P. Hövel, Phys. Rev. E **91**, 022917 (2015).
[22] S. Olmi, A. Politi, and A. Torcini, Europhys. Lett. **92**, 60007 (2010).
[23] G. C. Sethia, A. Sen, and G. L. Johnston, Phys. Rev. E **88**, 042917 (2013).
[24] A. Zakharova, M. Kapeller, and E. Schöll, Phys. Rev. Lett. **112**, 154101 (2014).
[25] J. Xie, E. Knobloch, and H.-C. Kao, Phys. Rev. E **90**, 022919 (2014).
[26] L. Schmidt and K. Krischer, Phys. Rev. Lett. **114**, 034101 (2015).
[27] Y. Suda and K. Okuda, Phys. Rev. E **92**, 060901(R) (2015).
[28] V. K. Chandrasekar, R. Gopal, D. V. Senthilkumar, and M. Lakshmanan, Phys. Rev. E **94**, 012208 (2016).
[29] F. P. Kemeth, S. W. Haugland, L. Schmidt, I. G. Kevrekidis, and K. Krischer, Chaos **26**, 094815 (2016).
[30] A. Mishra, S. Saha, P. K. Roy, T. Kapitaniak, and S. K. Dana, Chaos **27**, 023110 (2017).
[31] I. A. Shepelev, T. E. Vadivasova, A. V. Bukh, G. I. Strelkova, and V. S. Anishchenko, Phys. Lett. A **381**, 1398 (2017).
[32] A. M. Hagerstrom, T. E. Murphy, R. Roy, P. Hövel, I. Omelchenko, and E. Schöll, Nat. Phys. **8**, 658 (2012).
[33] M. R. Tinsley, S. Nkomo, and K. Showalter, Nat. Phys. **8**, 662 (2012).
[34] E. A. Martens, S. Thutupalli, A. Fourrière, and O. Hallatschek, Proc. Natl. Acad. Sci. USA **110**, 10563 (2013).
[35] T. Kapitaniak, P. Kuzma, J. Wojewoda, K. Czolczynski, and Y. Maistrenko, Sci. Rep. **4**, 6379 (2014).
[36] L. Larger, B. Penkovsky, and Y. L. Maistrenko, Phys. Rev. Lett. **111**, 054103 (2013).
[37] L. V. Gambuzza, A. Buscarino, S. Chessari, L. Fortuna, R. Meucci, and M. Frasca, Phys. Rev. E **90**, 032905 (2014).
[38] E. M. E. Arumugama and M. L. Spano, Chaos **25**, 013107 (2015).
[39] L. Larger, B. Penkovsky, and Y. Maistrenko, Nat. Commun. **6**, 7752 (2015).
[40] J. D. Hart, K. Bansal, T. E. Murphy, and R. Roy, Chaos **26**, 094801 (2016).
[41] J. Buck and E. Buck, Science **159**, 1319 (1968).
[42] S. Danø, P. G. Sørensen, and F. Hynne, Nature (London) **402**, 320 (1999).
[43] Z. Néda, E. Ravasz, Y. Brechet, T. Vicsek, and A.-L. Barabási, Nature (London) **403**, 849 (2000).
[44] P. Dallard, T. Fitzpatrick, A. Flint, A. Low, R. R. Smith, M. Willford, and M. Roche, J. Bridge Eng. **6**, 412 (2001).
[45] I. Kiss, Y. Zhai, and J. Hudson, Science **296**, 1676 (2002).
[46] Y. Kuang, *Delay Differential Equations with Applications in Population Dynamics* (Academic Press, Boston, 1993).
[47] T. Erneux, *Applied Delay Differential Equations* (Springer-Verlag, New York, 2009).
[48] V. I. Ponomarenko, D. D. Kul'minskii, A. S. Karavaev, and M. D. Prokhorov, Tech. Phys. Lett. **43**, 309 (2017).
[49] K. Ikeda and K. Matsumoto, Phys. D (Amsterdam, Neth.) **29**, 223 (1987).
[50] M. D. Prokhorov and V. I. Ponomarenko, Phys. Rev. E **72**, 016210 (2005).
[51] P. Clusella, A. Politi, and M. Rosenblum, New J. Phys. **18**, 093037 (2016).
[52] P. Ashwin and O. Burylko, Chaos **25**, 013106 (2015).
[53] I. Omelchenko, O. E. Omel'chenko, A. Zakharova, M. Wolfrum, and E. Schöll, Phys. Rev. Lett. **116**, 114101 (2016).
[54] A. Röhm, F. Böhm, and K. Lüdge, Phys. Rev. E **94**, 042204 (2016).
[55] Y. Maistrenko, S. Brezetsky, P. Jaros, R. Levchenko, and T. Kapitaniak, Phys. Rev. E **95**, 010203(R) (2017).